Ionization and Electron Transfer in Collisions of Two H Atoms: 1.25–117 keV*

G. W. McClure
Sandia Laboratory, Albuquerque, New Mexico
(Received 5 September 1967)

Cross sections for electron loss and electron capture by H atoms in encounters with H target atoms are measured in the energy range 1.25 to 117 keV. The electron loss process is measured for H on H_2 as a check on the method. Three methods of controlling the excited-state distribution of the H atom beam are investigated in the energy range 25 to 100 keV. One method achieves a nearly pure 1*s*-state beam. Results are compared with theoretical Born-approximation calculations by Bates and Griffing; the theoretical cross section for the ionization process is about 0.5 times the experimental value at 20 keV and equal to the experimental value at ~80 to 100 keV. The experimental values of the electron-capture cross section are a factor of 2.5 to 3 below Mapleton's Born calculations. The quantum-number dependence of the ionization cross section is deduced from a comparison of cross-section measurements obtained with the different beam-preparation methods. If the ionization cross section is assumed to vary as n^α, where n is the quantum number of the excited projectile atom and α is a constant, it is found that α lies between 0 and 1, with most probable values <0.36 for H on H_2 and <0.77 for H on H.

I. INTRODUCTION

THIS paper reports a study of conversion of an H atom projectile of keV energy into an H^+ or H^- ion in a single collision with another H atom of thermal energy. Three reactions can cause conversion of the projectile to an H^+ ion:

$$\begin{aligned} H+H &\rightarrow H^++H+e \quad \text{(reaction I)} \\ &\rightarrow H^++H^++2e \quad \text{(reaction II)} \\ &\rightarrow H^++H^- \quad \text{(reaction III)}. \end{aligned}$$

A single reaction can cause conversion of the projectile to an H^- ion:

$$H+H \rightarrow H^-+H^+ \quad \text{(reaction IV)}.$$

Denoting the cross sections for reactions I through IV by σ_I through σ_{IV}, one may define the measured quantities of this investigation as

$$\sigma^+(1)=\sigma_I+\sigma_{II}+\sigma_{III},$$
$$\sigma^-(1)=\sigma_{IV}.$$

Under the assumption $\sigma_{III}=\sigma_{IV}$, one may obtain $\sigma_I+\sigma_{II}$ from the difference $\sigma^+(1)-\sigma^-(1)$.

Several previous investigations have dealt with electron loss and capture by H atoms in gases other than atomic hydrogen. (See "note added in manuscript" at end of text.) Results have been recently compared and summarized by McClure[1] for H_2 gas and by Williams[2] for H_2, He, Ne, Ar, Kr, and Xe gases. Measurements have also been obtained on N_2, O_2, NO, and CO gases.[3–6]

As a test of the experimental technique, we have repeated cross-section measurements for the reaction

$$H+H_2 \rightarrow H^++H_2+e \quad \text{(reaction V)}.$$

An additional incentive for repeating this measurement is that this cross section is needed in order to correct the present data for effects of residual H_2 in the collision chamber. The cross section for the companion reaction

$$H+H_2 \rightarrow H^-+H_2^+, \quad \text{(reaction VI)},$$

needed for corrections in calculating $\sigma^-(1)$, was taken from earlier work.[1] We have also determined the angular spread of the post-collision H^+ and H^- ions from H atoms incident on both H and H_2 targets. The results suggest a possible explanation for a discrepancy between our results[1] and those of Williams[2] at low energies.

Experiments were performed using several different means of preparation of the H beam in order to vary the population of excited states. One of the methods produces projectiles essentially in the 1*s* ground state. Comparison of results obtained using different beam preparation schemes permits us to estimate the dependence of the ionization cross section on the principal quantum number of the incident H atom. Previous results on this question, obtained by Riviere and Sweetman,[7] have pertained to the 14th quantum level and were obtained by a quite indirect method. Attention to the quenching of the 2*s* metastable state in the H beam has been given in previous work on $H+H_2$ collisions,[1,2] and the effect on the cross section was shown to be small.

For collisions of 1*s* atoms, theoretical calculations have been carried out by Bates and Griffiing[8] of the

* This work was supported by the U. S. Atomic Energy Commission.

[1] G. W. McClure, Phys. Rev. **134**, A1226 (1964).
[2] J. F. Williams, Phys. Rev. **153**, 116 (1967).
[3] P. M. Stier and C. F. Barnett, Phys. Rev. **103**, 896 (1956).
[4] R. Curran and T. M. Donahue, Phys. Rev. **118**, 1233 (1960).
[5] D. V. Pilipenko and I. M. Fogel, Zh. Eksperim. i. Teor. Fiz. **42**, 936 (1962) [English transl.: Soviet Phys.—JETP **15**, 646 (1962)].
[6] D. V. Pilpenko and I. M. Fogel, Zh. Eksperim. i Teor. Fiz. **44**, 1818 (1963) [English transl.: Soviet Phys.—JETP **17**, 1222 (1963)].
[7] A. C. Riviere and D. R. Sweetman, in *Atomic Collision Processes*, edited by M. R. C. McDowell (North-Holland Publishing Co., Amsterdam, 1964), p. 734.
[8] D. R. Bates and G. W. Griffing, Proc. Phys. Soc. (London) **A68**, 90 (1955).

sum of the cross sections for reactions I and II. Comparison of the theoretical and experimental results is made as a test of the accuracy of the Born approximation. The only previous comparison of theory and experiment for neutral-neutral ionizing collisions is for the case of H+He.[9] (See "note added in manuscript" at end of text.)

The present results provide a test of the theoretical "post" and "prior" Born-approximation calculations of Mapleton[10] for the electron-transfer reaction IV.

II. METHOD

This investigation entails the production of an H atom beam by proton charge exchange in H_2 gas, the separation of unconverted protons from the neutral beam, the processing of the neutral beam by a variable drift path in a variable applied field, the passage of the processed H beam through a collision chamber in which H_2 gas is catalytically dissociated yielding a high (80%) concentration of atomic hydrogen, the separation of the beam emergent from the collision chamber into H^+, H, and H^- beams, and the measurement of the particle fluxes in each of these beams by a proportional counter detector.

The production of an H beam by charge exchange has been used in previous investigations referred to in Sec. I to study electron capture and loss by H atoms in other gases. Charge-exchange–cell gases, gas pressures, and path lengths have, however, varied from one investigation to another, undoubtedly causing some variation in the population of excited states within the neutral beam.

The processing of the neutral beam in the present experiment incorporates three distinct methods: (1) an 8-cm drift path which permits the decay of the low-lying excited states having relatively short lifetimes; (2) a 111-cm drift path which considerably extends toward higher quantum numbers the group of quantum states which decay in flight; and (3) a strong electric field which ionizes[7] virtually all atoms which do not decay radiatively in 111 cm.

An atomic-hydrogen target of the general type used here was first employed by Lockwood and Everhart,[11] and a modified version with improved electrical connections and simplified construction has been used in this laboratory for several investigations.[12,13] Data are obtained at each beam energy with the target chamber at two standard temperatures of 2373 and at 295°K and at two standard H_2 gas flow rates following the method used in previous work.[12,13]

The ratio of H_2 molecule concentration at the high temperature to that at the low temperature, denoted A, is obtained[14] by observing the H^- yield at an H^+ energy of 20 keV from the reaction

$$H^+ + H_2 \rightarrow H^- + 2H^+ \quad \text{(reaction VII)}.$$

This ratio is observed easily without modification of the apparatus. The ratio of the concentration of H atoms in the target chamber (free atoms counted once and H_2 molecules counted twice) at the high temperature to that at the low temperature is denoted by B and is determined[14] by measurements of Coulomb scattering of 20-keV protons to an angle of $\sim$14 mrad. Both of these schemes were suggested by Lockwood, Helbig, and Everhart[15] and both have been used in our previous work[12] to assess the gas target conditions. Reference 12 contains a detailed discussion of the method employed.

Calibration of the target gas thickness at a temperature of 295°K (H_2 gas undissociated) is accomplished by observing fractional conversion of H^+ to H in the reaction

$$H^+ + H_2 \rightarrow H + H_2^+ \quad \text{(reaction VIII)}$$

at 10 keV. The calibration is based on the assumption that reaction VIII has a cross section of 8.8×10^{-16} cm^2. This value was obtained in a measurement based on Coulomb scattering calibration[12] and is thought to be more accurate than the value 8.2×10^{-16} cm^2 used in previous work.[1,2]

The following symbols are employed in the discussion of the data:

(1) $\sigma^+(1)$ is the cross section per target gas atom for conversion of an H projectile atom to an H^+ ion via reactions I, II, and III;

(2) $\sigma^-(1)$ is the cross section per target gas atom for conversion of an H projectile atom to an H^- ion via reaction IV;

(3) $\sigma^+(2)$ is the cross section per target gas molecule for conversion of an H projectile atom to an H^+ ion via reaction V;

(4) $\sigma^-(2)$ is the cross section per target molecule for conversion of an H projectile atom to an H^- ion via reaction VI. [It is necessary to consider the values of $\sigma^+(2)$ and $\sigma^-(2)$ only in order to correct for the residual H_2 in the collision chamber at the higher standard collision-chamber temperature 2373°K];

(5) $N^+(T_i)$ is the change in number of protons emergent from the collision chamber per incident H atom when the gas flow is switched from high to low standard flow rate at collision-chamber temperature T_i;

(6) $N^-(T_i)$ is the change in the number of H^- ions emergent from the collision chamber per incident H atom when the gas flow is switched from high to low standard flow rate at collision-chamber temperature T_i;

[9] D. R. Bates, in *Atomic and Molecular Processes*, edited by D. R. Bates (Academic Press Inc., New York, 1962), p. 569.
[10] R. A. Mapleton, Proc. Phys. Soc. (London) **85**, 841 (1965).
[11] G. J. Lockwood and E. Everhart, Phys. Rev. **125**, 567 (1962).
[12] G. W. McClure, Phys. Rev. **148**, 47 (1966).
[13] G. W. McClure, Phys. Rev. **153**, 182 (1967).
[14] The ratios A and B are defined precisely in Ref. 12.
[15] G. J. Lockwood, H. F. Helbig, and E. Everhart, J. Chem. Phys. **41**, 3820 (1964).

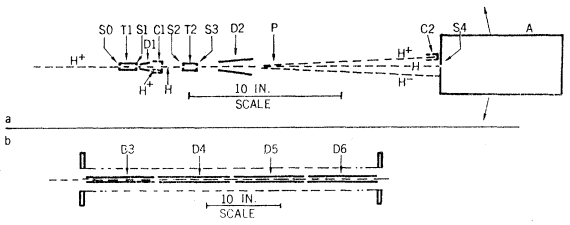

FIG. 1. (a) Apparatus diagram. *T*1—neutralizing chamber, *D*1—electrostatic deflection plates, *C*1—Faraday cup, *T*2—heated collision chamber, *D*2—electrostatic deflection plates, *C*2—Faraday cup, *A*—proportional counter detector. *S*0, *S*1, *S*2, *S*3—circular apertures having diameters of 0.010, 0.030, 0.010, and 0.080 in., respectively. *S*4—rectangular slit 0.001 in. wide in direction parallel to plane of figure, and 0.963 in. wide in direction perpendicular to plane of figure. Arrows indicate direction of motion of *A* about rotation center *P* permitting stepwise scanning of H^+, H, and H^- beams to determine intensity ratios and angular distributions. Walls of *T*2 are made of 0.001-in. tungsten, heatable by electrical conduction to 2373°K. All parts except the interior of *A* are surrounded by 4-in.-diam vacuum vessels pumped by two 400-liter/sec diffusion pumps. *T*1 and *T*2 have separate H_2 gas supplies not shown. Gimbals at *S*0 and *P* permit alignment of component sequence *S*0 through *D*2 relative to incoming beams and motion of counter *A* for beam scanning. (b) Drift tube inserted between *C*1 and *S*2 for beam processing by methods 2 and 3. *D*3, *D*4, *D*5, and *D*6—deflection plates to which voltages are applied in method 3. *D*3 plate spacing is 0.040 in. *D*4, *D*5, and *D*6 spacing is 0.130 in. A 200-liter/sec diffusion pump evacuates the tube housing components *D*3 to *D*6.

(7) $T_a=295$°K is the lower standard temperature;
(8) $T_b=2373$°K is the higher standard temperature;
(9) N^0 is the change in the number of H atoms emergent from the collision chamber per incident H^+ ion (reaction VIII) when the gas flow is switched from high to low standard flow rate. This is measured only at temperature T_a;
(10) $K=8.8\times10^{-16}$ cm$^2/N^0$ is the target calibration constant;
(11) A is the ratio defined above;
(12) B is the ratio defined above.

Following the measurement of N^0, $N^+(T_a)$, $N^+(T_b)$, $N^-(T_b)$, A, and B, the cross sections were determined from the formulas

$$\sigma^+(1)=K\frac{N^+(T_b)-AN^+(T_a)}{2(B-A)}, \quad (1)$$

$$\sigma^-(1)=K\frac{N^-(T_b)-AN^-(T_a)}{2(B-A)}, \quad (2)$$

$$\sigma^+(2)=KN^+(T_a), \quad (3)$$

$$\sigma^-(2)=KN^-(T_a). \quad (4)$$

The ratio $\sigma^-(2)/\sigma^+(2)$ was taken from our previous results[1] so that $N^-(T_a)$ could be calculated from $N^+(T_a)$ and with the aid of the equation $N^-(T_a)/N^+(T_a)=\sigma^-(2)/\sigma^+(2)$ derived from Eqs. (3) and (4).

These formulas are easily derived with the assumption that the probabilities of H atom conversion to H^+ or H^- in the slit edges and in residual gases in the collision to H^+ or H^- in the slit edges and in residual gases in the collision chamber are the same at the two standard gas-flow rates at a given collision-chamber temperature. A dependence of these probabilities on temperature would not affect the validity of the equations.

III. APPARATUS

A schematic diagram of the apparatus is shown in Fig. 1. The H^+ beam incident from the left is produced by a simple ion accelerator[12] with a magnetic analyzer providing a pure proton beam free from other ions and having an energy spread of less than 1% of the mean ion energy.[12] Neutralizing chamber *T*1 contained H_2 gas at a pressure of 10^{-4} mm Hg which was admitted through a slow leak. The pressure in this chamber was monitored by observing the pressure drop along a section of the gas feed line with an MKS Baratron capacitance manometer. Neutrals produced in *T*1 proceeded directly toward aperture *S*2 of the main collision chamber *T*2, while protons which were not neutralized were deflected into the corner of Faraday cup *C*1. The proton current from *C*1 was integrated and used to control the mechanical drive of the counter *A* in stepwise fashion across any of the three beams emergent from *T*2 during beam intensity determination. This feature minimized variations in the data associated with accelerator beam instability.

The collision chamber *T*2 was exactly the same as that employed in previous work.[12,13] Input and output apertures *S*2 and *S*3 were designed to permit any secondary H^+ or H^- ion or scattered H atom produced within an angle of 44 mrad of the main beam to emerge from *S*3. All emergent particles within this angular range passed between deflection plates *D*2 toward the detector slit *S*4. The detector-slit length in the direction normal to the diagram was sufficient to intercept all particles emergent from the collision chamber at angles within ±31 mrad of the plane of the figure. The available detector scan range was ample to cover all beam widths encountered in these experiments and the deflector voltage available on plates *D*2 was sufficient to separate the H^+, H, and H^- beams at the detector entrance plane.

The proportional counter detector has been described previously.[16] Its most important characteristic for the present work was its ability to count individually the H^+, H, and H^- particles entering its window and to respond with equal efficiency to all three of these particles at a given energy. This equality in efficiency results from the fact that both the counter window and the counter gas have thicknesses of many charge-exchange mean free paths and the scattering in one charge-exchange mean free path is small. Consequently, an incident particle of any of these types loses its

[16] G. W. McClure and D. Allensworth, Rev. Sci. Instr. **37**, 1511 (1966).

charge-state identity before undergoing any appreciable scattering.

The upper part of Fig. 1 shows the apparatus arrangement with which most of the data were obtained. Here the drift path length between $S1$ and $S2$ was only 8 cm. In some measurements the 103-cm drift tube diagrammed in Fig. 1(b) was inserted between $C1$ and $S2$.

The use of four sets of plates was decided upon in order to provide flexibility in beam processing. Because the changes in the observed cross section caused by gross changes in beam processing were comparable to the experimental uncertainties, detailed investigations of the effects of electric field in the 103-cm tube were not made.

High-speed diffusion pumps extracted gas from the long drift section [Fig. 1(b)] and from all regions surrounding the two collision chambers $T1$ and $T2$. The pressures in these regions were always less than 2×10^{-7} mm Hg. Corrections for beam attenuation and charge exchange in the drift spaces were negligible compared to the statistical spread in successive beam-flux determinations.

Gas feed to chamber $T2$ was made through a Pd leak rather than a Ni leak as in previous work.[12,13] No change was observed in the quantities A or B as a result of this modification. As before, gas flow into $T2$ was monitored by means of an MKS Baratron differential capacitance manometer which indicated the pressure drop along a short section of the H_2 gas feed line to chamber $T2$.

IV. OPERATING CONDITIONS

The higher and lower standard flow rates of H_2 gas into chamber $T2$ were such as to yield partial pressures of 5×10^{-4} Torr and 10^{-5} Torr, respectively, in $T2$ as calculated from estimates of the conductivity of the gas-flow system. This result checked satisfactorily with the target thickness inferred from the measurement of N^0 and the value assumed for the cross section for reaction VIII. Generally, the ratio of the secondary particle yields recorded in changing from high to low standard flow rates was less than the ratio of 50 expected from the pressure change. The discrepancy was probably due to secondaries produced in the slit edges of $S2$ or in residual gas in the collision chamber. These spurious secondaries were prevented from influencing the cross sections by using differences of particle yields obtained at the two standard flow rates for all yield determinations.

During each beam scan by detector A, an angular distribution was automatically recorded. Figure 2 displays several of the scan records showing the width of the H^+ beam from reactions I, II, and III as well as the pressure effect on the yield of H^+. Scan widths were always chosen to reduce the ignored parts of the beam to a negligible level. The scan widths required to encompass the beams varied from ~0.080 in. at 117 keV

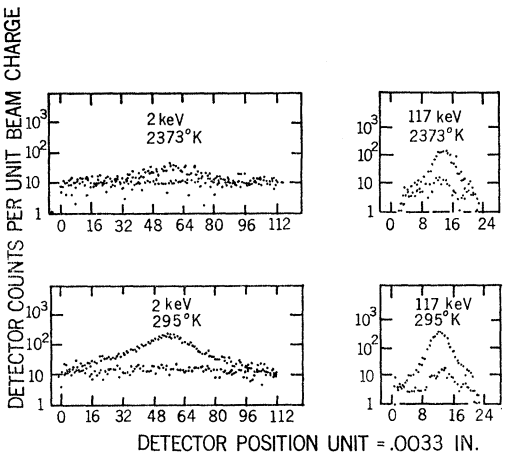

FIG. 2. Detector H^+ counts per unit proton change collected at cup $C1$ versus horizontal position of slit $S4$. H^- beam widths were comparable to these. H primary beam width was much narrower (about 6 units full width at half-maximum). Upper sets of points in each picture were obtained with higher standard gas-flow rate of H_2 into $T2$ and lower set with lower standard flow rate of H_2 into T_2. Lower points represent mainly background from slit-edge scattering at $S2$ and scattering from residual gases ahead of plates $D2$.

to 0.33 in. at 1.2 keV. These widths corresponded to angles of secondary-particle production of from 2.5 to ~10 mrad. Both of these angles are considerably smaller than the angles subtended by the detector slit height and the aperture $S3$ for particles originating at all points along the beam path in $T2$.

The neutral beam intensity at the detector was shown to be a linear function of the pressure in $T1$. This gave assurance that the primary neutrals were produced in single collisions in the gas in $T1$ and not in the slit edges or elsewhere along the beam path. This point is relevant since data on electron capture in H_2 were used to estimate the excited-state population in the beam of H atoms emergent from $S1$. The population is undoubtedly dependent on the production mode.

At each beam energy, the proton beam entering $S0$ was adjusted so that the H atom counting rate at $S4$ was 10^3 to 10^4/sec at the center of the H atom beam scan. At these rates H atom count losses due to pile-up were negligible, and rates of 10/sec to 100/sec were recorded in the central portions of the H^+ and H^- secondary beams at the higher standard rate of gas flow into $T2$. Proton currents into cup $C1$ were of the order of 10^{-10} to 10^{-13} A depending on the efficiency of electron capture in $T1$, which varied strongly with energy.

Values of constants A and B determined at three different times during the course of the investigation were mutually consistent and agreed with values measured in two previous investigations with the same standard operating temperatures and gas-flow rates. The mean values obtained in the present set of measurements were $A=0.063\pm0.005$ and $B=0.290$

TABLE I. Methods employed to process H atom beam between neutralizing chamber and collision chamber.

Method 1:	0.3-cm drift before reaching deflection plates $D1$, 2.4-cm drift in field of deflection plates $D1$, 5.8-cm drift between exit from $D1$ and arrival at collision chamber. The field in $D1$ decreases linearly by a factor of 3 from the entrance to the exit. The value of the field at the midpoint of $D1$ was $35.9E$ V/cm, where E is the H atom energy in keV. (By maintaining a fixed ratio between beam energy and deflection voltage, the proton beam emergent from $S1$ was directed to the same spot in $C1$, independent of proton energy.)
Method 2:	Same as method 1, except for the addition of 103-cm field-free drift space to the 5.8-cm gap following $D1$.
Method 3:	Same as method 2, except for the addition of voltages to deflection plates $D3$ to $D6$ such that a 100-keV/cm field was applied to the beam for a length of 25 cm starting 3.4 cm from $D1$ and a 3-keV/cm field was applied for the next 75 cm. The beam then entered the collision chamber after a 6-cm field-free drift.

± 0.006, where the indicated uncertainties are standard deviations.

V. BEAM PREPARATION

In this section a general discussion is presented of the factors which influence the excited-state population of the H atom beam arriving at the entrance to the collision chamber. Calculated populations will be shown for each of the three beam-preparation methods employed in the experimental study enumerated in Table I. Finally, calculated results are shown for the ratios of the ionization cross sections obtained for each of the three beam-preparation methods relative to the ground-state cross section, assuming that the ionization cross section of a beam atom in collision with a target atom or molecule varies as the 0.25, 0.5, or 1.0 power of the principal quantum number. Comparison of these last results with the experimental data permits one to infer the approximate strength of the quantum number dependence of the ionization cross section.

The atoms emergent from the neutralizing chamber $T1$ possess a quantum-number distribution characteristic of the energy of the entering H^+ ions and the gas used in the charge-exchange chamber. In the present case, the gas is H_2 and the target is thin so that single-collision conditions prevail. The experimental data of Hughes,[17] together with total-cross-section data,[12] show that for capture into states $1s$, $3s$, and $4s$ the capture cross section varies as n^{-3} at 100 keV. The results of Riviere[7] giving the ratio of the cross section for capture into the $n=14$ level to the total cross section confirm this dependence. The Bates and Dalgarno[18] Born-approximation calculation of electron transfer to protons in atomic hydrogen also predicts an n^{-3} dependence for s states with n in the range 1 through 4. A similar theoretical dependence is found[18] for p and d states in the same range of n values. On the basis of the above information, we generalize as follows:

$$\sigma_c = A_l n^{-3},$$

where σ_c is the capture cross section for H^+ in H_2, A_l is a constant for each angular momentum l, and n is the principal quantum number. Following the theoretical result[18] at 100 keV, we assume that $A_1 = A_0$, $A_2 = 0.1\ A_0$, and $A_{l\geq 3} \ll A_0$. The population given by these expressions will represent to a good approximation the beam condition at the exit aperture $S1$ at 100 keV, except for the $2p$ state which decays to a negligible level in the drift space beyond $S1$ with all beam-preparation methods.

The decay of the various quantum states in the region of deflection plates $D1$ is influenced by the Stark-effect perturbation of energy levels and eigenfunctions. In order to deduce the lifetime of states in the high-field regions, we refer to the calculations presented by Bethe and Salpeter.[19] At 100 keV the field in region $D1$ varied

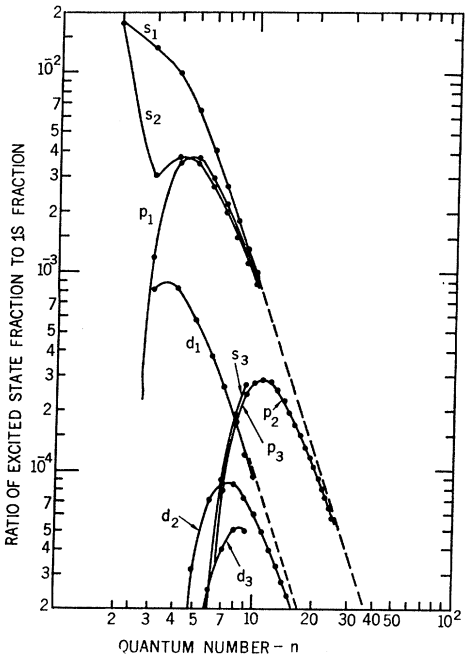

FIG. 3. Calculated excited-state populations of H atom beam entering collision chamber $T2$ for the three beam-preparation methods listed in Table I and for protons of energy 100 keV. Labels s, p, and d refer to orbital angular momentum; subscripts 1, 2, and 3 refer to beam preparation methods 1, 2, and 3; and n refers to principal quantum number of excited state. Curve p_3 coincides with p_2 for $n \leq 9$, but $p_3 = 0$ for $n \geq 10$. Fractions s_3 and d_3 are also zero for $n \geq 10$. Fractions s_1 and s_2 are equal for $n=2$ because the $2s$ quantum state is metastable and unaffected by the addition of the long tube with zero field in method 2. States of higher angular momentum than d states are not significantly populated.

[17] R. H. Hughes, H. R. Dawson, B. M. Daughty, D. B. Kay, and C. A. Stigers, Phys. Rev. **146**, 53 (1966). Data on the $4s$ state were obtained from R. H. Hughes (private communication).

[18] D. R. Bates and A. Dalgarno, Proc. Phys. Soc. (London) **A66**, 972 (1953).

[19] H. A. Bethe, and E. E. Salpeter, *Quantum Mechanics of One- and Two-Electron Atoms* (Academic Press Inc., New York, 1957).

from 5400 to 1780 V/cm because the plates were tilted slightly. However, the field throughout the region is sufficiently high that the $2S_{1/2}$ and $2P_{1/2}$ states are strongly mixed and the effective decay rate of the $S_{1/2}$ metastable state is 3.5×10^8/sec. The $2P_{1/2}$ and $2P_{3/2}$ levels were assumed to retain their natural field-free lifetimes in this region. This is not quite accurate, but these levels are so strongly attenuated in $D1$ and the remaining 5-cm drift space that any reasonable decay rate leads to a negligible contribution from these states. We assume that the $3S_{1/2}$ and $3P_{1/2}$ levels have decay rates in $D1$ equal to the field-free value for $3P_{1/2}$ and we assume all $3D$ levels have decay rates equal to 1.25×10^8/sec. This rate is the highest of the values given by Bethe and Salpeter for quantum levels $n=3$ in a strong electric field.[20] For levels with $n\geq3$ and fixed l, we assume decay rates varying as n^{-3}.

In beam-preparation method 2, we apply no voltages to the deflection plates in the 103-cm drift tube. In addition, the tube is shielded magnetically so we can assume that all states decay at their normal field-free rates throughout the long tube.

In beam-preparation method 3, the first set of plates $D3$ has a field of 100 keV/cm which will field-ionize[7] all quantum states having $n\geq10$ leaving only states with $n<10$ to enter collision chamber $T2$. The surviving states are assumed to have the following decay rates throughout the long tube in both the 100-keV/cm region $D3$ and the 3-keV/cm regions $D4$ through $D6$: $2S_{1/2}$ and $2P_{1/2}$ decay rates equal the normal field-free rate of $2P_{1/2}$, and $3D$ states decay at the rate 1.25×10^8/sec as assumed for region $D1$. Here again, all higher quantum states are assumed to decay at rates proportional to n^{-3} for a given l. Under these assumptions and with the neglect of cascading, the populations of excited states arriving at $T2$ are as shown in Fig. 3. It is evident that the three preparation methods lead to drastically different populations.

An estimate was made of the dependence of the average ionization cross section σ_{av} on the beam-preparation method by assuming an ionization cross section of the form

$$\sigma=\sigma(1s)n^{\alpha},$$

where $\sigma(1s)$ is the ionization cross section for a projectile H atom in the $1s$ state, n is the principal quantum number of the projectile atom state, and α is a constant. For several values of α the above equation was averaged over the distributions shown in Fig. 3. The results are shown in Table II.

TABLE II. Calculated ratio of the average ionization cross section σ_{av} to cross section $\sigma(1s)$ for ionization of atoms in $1s$ state for the three different beam-preparation methods (Table I) and for three assumed dependences of ionization cross sections on principal quantum number of H atoms of the form $\sigma=\sigma(1s)n^{\alpha}$ (for 100-keV beam energy).

Beam-preparation method	Cross section ratio $\sigma_{av}/\sigma(1s)$ $\alpha=0.25$	$\alpha=0.50$	$\alpha=1.0$
1	1.028	1.0801	1.33
2	1.016	1.045	1.21
3	1.0005	1.0017	1.0068

[20] Reference 19, Table 20a, p. 277.

TABLE III. Cross section $\sigma^+(2)$ for reaction V for the three beam-preparation methods listed in Table I (in units of 10^{-17} cm^2/molecule).

E (keV)	Method 1	Method 2	Method 3
100	10.79±0.25	11.35±0.09	10.89±0.09
80	12.62±0.24	12.23±0.13	
63	13.04±0.33	14.02±0.35	13.79±0.20
50	15.29±0.47	15.00±0.09	
40	15.16±0.39	15.32±0.11	
31.5	14.34±0.30	14.67±0.25	
25	14.18±0.37	13.89±0.15	

It is seen that any of the three α values leads to less than 1% excess of σ_{av} over $\sigma(1s)$ with beam-preparation method 3, whereas the larger α values 0.5 and 1.0 lead to substantial excesses between 4 and 33% of σ_{av} over $\sigma(1s)$ with beam-preparation methods 1 and 2. Based on the experimental results, we will attempt to roughly estimate α.

VI. RESULTS

Table III summarizes all determinations of cross section $\sigma^+(2)$ at those beam energies in which more than one beam-preparation method was used. These studies were made only at the higher energies because the relative probability of levels with $n>1$ being populated in the neutralizing chamber is theoretically greater at high energies and because the probability for such states to decay in flight after leaving $T1$ is least at high energies. Hence, any excited-state effects were expected to be at a maximum at high energies.

From Table III it may be seen that at both 100 keV and 63 keV the over-all effect on $\sigma^+(2)$ caused by changing the drift path from 8 cm with no field ionization to 111 cm with field ionization (first and last columns) is 4 to 7% and is of the same order of magnitude as the experimental errors. At all energies from 25 to 100 keV no significant change in $\sigma^+(2)$ is introduced by changing the H atom drift path from 8 to 111 cm (first and second columns). At a few energies the cross-section values are larger when the path length is larger. This is thought to be a statistical fluctuation, rather than a real effect, since to explain such an effect in terms of excited-state populations would require a lower ionization cross section for an excited state than for the $1s$ state.

Corresponding results for $\sigma^+(1)$ are shown in Table IV. The value for the long-tube "high-field" case is about 11% below the short-tube value, but the probable error in the ratio is 8% so that one cannot be confident that the ratio is different from 1. Further measurements of $\sigma^+(1)$ for various beam preparations were not made

TABLE IV. Cross section $\sigma^+(1)=\sigma_I+\sigma_{II}+\sigma_{III}$ for the three beam-preparation methods listed in Table I (in units of 10^{-17} cm²/molecule).

E (keV)	Method 1	Method 2	Method 3
100	6.13±0.32	6.35±0.50	5.5±0.33

because of the large expenditure of time that would be required to reduce the experimental uncertainties in $\sigma^+(1)$ enough to obtain statistically significant evidence of an excited-state effect.

The ratios of the cross-section values in the various columns of Tables III and IV were calculated and compared with data in Table II in order to estimate the power of α in the ionization cross-section dependence which would represent the present data. Of the 11 independent ratios obtainable from Table III, six imply negative values of α. The remaining five cases imply values of α in the range 0.2 to 0.44. The latter have an average of 0.36. The over-all average, including the negative values, would be less than 0.36. Of the three ratios available from Table IV, one gives a negative α and the other two give values of 0.9 and 0.64 averaging 0.77. The average including the negative value would be less than 0.77.

No theoretical estimates are available of the appropriate value of α for H+H or H+H_2 collisions. Omidvar's calculations[21] for e+H collisions indicate that the theoretical value of α which represents the n dependence of the H atom ionization cross section is about 2.0. Apparently, then, the neutral-neutral case is quite different from the charged-neutral case. Riviere and Sweetman[7] have obtained results on the ionization of the 14th quantum level of H in H_2 collisions which are consistent with the present findings.

In Table V are presented the composite values $\sigma^+(1)$, $\sigma^-(1)$, and $\sigma^+(2)$. The $\sigma^+(2)$ values shown for E>25 keV are averages of the values obtained by methods 1 and 2. Results for these two methods did not differ significantly. The values of $\sigma^+(2)$ for $E<25$ keV were obtained entirely by method 1 and all of the $\sigma^+(1)$ and $\sigma^-(1)$ data were obtained by method 1. These results are shown graphically in Figs. 4 and 5 for comparison with other data. The agreement of the present $\sigma^+(2)$ values with those obtained previously,[1] seen in Fig. 4, lends support to the reliability of the experimental procedure. The data on $\sigma^-(2)$ are from our previous work.[1] [The ratio $\sigma^-(1)/\sigma^+(2)$ from the 1964 measurements was used in the calculations of $\sigma^-(1)$ as described in Sec. II.]

The present results on $\sigma^+(2)$ agree with those of Stier and Barnett[3] at nearly all energies in the range 4 to 117 keV covered by both experiments. Stier and Barnett's data fall 11% above ours at ~ 6 keV and 8% above ours at ~20 keV. Disagreements between our results and those of other investigators, particularly below 10 keV, can be seen by reference to more complete data presentations already given.[1,2]

There is a good agreement between the present $\sigma^+(2)$ data presented and the results of Williams[2] at energies from 8 to the 50-keV upper limit of Williams's data. At lower energies Williams's results gradually diverge from ours toward values about 0.65 times ours at 2 keV. The 2-keV angular distribution shown in Fig. 2 shows that some secondary H atom losses will be encountered in a measurement where H atoms produced at angles of 2.5 mrad (13 position units in Fig. 2) from the beam axis are rejected. An inspection of the geometry of Williams's collision chamber suggests that such rejection was occurring owing to aperture-size selection. This accounts for at least a part of the discrepancy at low energies.

In Fig. 5 the experimental values of $\sigma^+(1)$ and $\sigma^-(1)$ are shown together with the difference between the two quantities, which is equal to $\sigma_I+\sigma_{II}$. The Born-approximation calculation of Bates and Griffing[8] is to be compared with the difference curve. It is seen that the theory and the experimental results agree at 100 keV. The long-tube, high-field value of $\sigma^+(1)$ from Table IV is seen to fall about 10% below the theory at 100 keV. The latter is considered to be a more valid comparison than the former, because the H beam in the latter case is essentially in the ground state. At energies below 70 keV a significant discrepancy between theory and experiment is present. The discrepancy becomes largest at 20 keV, where the experimental value of $\sigma^+(1)-\sigma^-(1)$ is 1.91±0.10 times the theoretical value.

The measured cross section $\sigma^-(1)$ for reaction III (or IV) is a factor of of 2.5 to 3 below the "post" and "prior" Born-approximation calculations of Mapleton.[10]

TABLE V. Cross sections $\sigma^+(2)$ obtained by methods 1 and 2 (Table I), and cross sections $\sigma^+(1)$ and $\sigma^-(1)$ obtained by method 1 (Table I).

E (keV)	$\sigma^+(2)$ (10^{-17} cm²/molecule)	$\sigma^+(1)$ (10^{-17} cm²/atom)	$\sigma^-(1)$ (10^{-17} cm² atom)
1.25	3.68±0.21	0.29±0.27	
1.6	5.12±0.29	1.37±0.20	
2.0	6.75±0.27	1.86±0.20	
2.5	8.35±0.47	2.42±0.23	
3.15	8.80±0.22	3.40±0.39	0.47±0.11
4.0	8.67±0.35	3.85±0.27	0.36±0.12
5.0	8.64±0.35	4.59±0.27	0.67±0.13
6.3	7.76±0.31	5.13±0.29	0.72±0.13
7.4			1.07±0.17
8.0	8.15±0.33	6.21±0.34	1.04±0.13
10.0	8.51±0.28	7.71±0.42	1.14±0.13
12.5	9.23±0.37	8.97±0.48	1.62±0.19
16.0	11.18±0.45	10.62±0.57	1.61±0.18
20.0	12.06±0.68	12.06±0.85	1.58±0.16
25.0	14.05±0.51	11.22±0.81	1.29±0.14
31.5	14.51±0.52	10.35±0.57	0.99±0.12
40.0	15.25±0.55	9.64±0.71	0.49±0.09
50.0	15.16±0.55	8.65±0.65	0.32±0.06
63.0	13.52±0.49	7.51±0.57	0.24±0.05
80.0	12.42±0.45	6.74±0.51	
100.0	11.25±0.24	6.13±0.32	
117.0	9.94±0.56	5.61±0.43	

[21] K. Omidvar, Phys. Rev. **140**, 26 (1965).

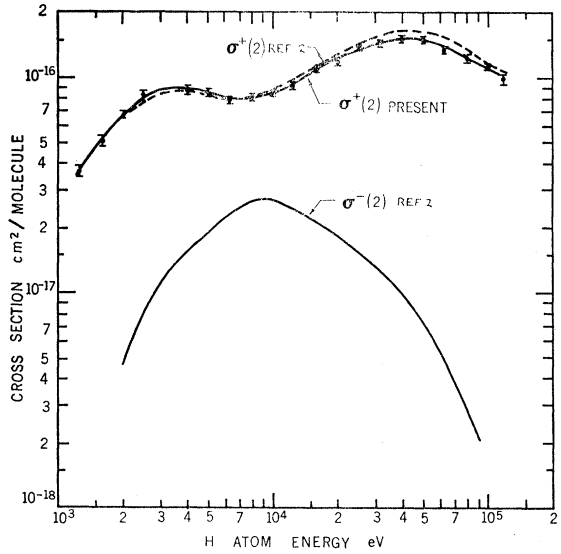

FIG. 4. Present measurement of $\sigma^+(2)$ for reaction V compared with earlier results reported in Ref. 2. The latter are renormalized to correspond to the same basis of calibration as used in the present experiment. (Assumption of cross section 8.8×10^{-16} cm² for reaction VIII at 10 keV.) $\sigma^-(2)$ cross-section data for reaction VI are also from Ref. 2 and are similarly renormalized.

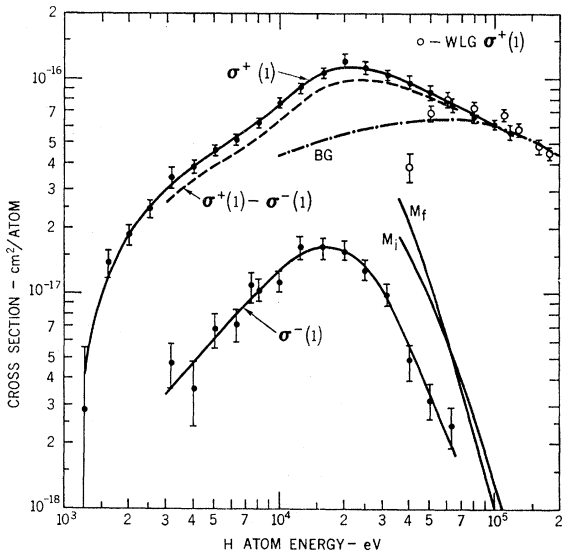

FIG. 5. Experimental results for $\sigma^+(1)$; the combined cross section for reactions I, II, and III. Also shown are experimental results for cross section $\sigma^-(1)$ for reaction IV. The difference curve (dashed) represents the total cross section for reactions I and II uncorrected for excited states. Curve BG is the Bates and Griffing theoretical result for the cross section for reactions I and II for 1*s* atoms. $\sigma^+(1)$, corrected for excited states, is about 10% below the solid curve at 100 keV. Curves M_i and M_f are the "post" and "prior" theoretical curves of Mapleton for reaction IV. The open circle are the experimental points of Whittkower *et al.* (see "note added in manuscript" at end of text).

This discrepancy is far outside the limits of experimental error. It is perhaps significant that the shapes of the experimental and theoretical curves are somewhat similar despite the discrepancies in cross-section magnitude.

We did not examine the effect of beam excitation on the cross section $\sigma^-(1)$. When the target atom is in the ground state and the projectile atom is in the nth quantum level, the reaction is endothermal with energy defects 12.9, 2.7, and 0.8 eV for $n=1$, 2, and 3, respectively, and is exothermal with energy excess of 0.1, 0.2, and 0.4 for $n=4$, 5, and 6, respectively. It is possible that the near resonant cases $n=3$, 4, and 5 have abnormally large electron transfer cross sections. If this is true, the experimental values of $\sigma^-(1)$ may be higher than the ground-state values in the neighborhood of 20 to 100 keV, where the beam fractions of the quantum state $n=3$ to 5 are appreciable as seen in Fig. 3, curves s_1, p_1, and d_1. Correction for this effect would be in such a direction as to worsen the gap between the Mapleton theoretical results[10] and the $\sigma^-(1)$ experimental data. The same effect would increase $\sigma^+(1)-\sigma^-(1)$, tending to worsen the disagreement with the Bates and Griffing results[8] in the same energy range.

Note added in manuscript. A. B. Whittkower, G. Levy, and H. B. Gilbody [Proc. Phys. Soc. (London) **91**, 306 (1967)] have also measured $\sigma^+(1)$. Their results are plotted in Fig. 5 for comparison with the present data. The discrepancies at 40 and 50 keV are outside the range of estimated uncertainties. Everhart [this issue, Phys. Rev. **166**, 68 (1968)] has undertaken scattering measurements in collisions of two H atoms.

ACKNOWLEDGMENTS

James M. Peek and Thomas A. Green contributed many stimulating discussions concerning the theoretical aspects of this study. D. L. Allensworth constructed the apparatus and performed the measurements with skill and patience. James M. Hesse supplied a purified solvent for counter-window preparation. R. H. Hughes graciously provided new data on capture into the 4*s* state.